

Experimental Study on CT Micro Mechanics Characteristics of Soft Rock Creep under Gravity Disturbance Loads

FU Zhiliang¹, GUO Hua² and GAO Yanfa³

Summary

This paper is focused on the micro-damage evolution properties of gray green mudstone under impacting disturbance load conditions for the first time by using the real time CT testing technique. CT images and CT values for rock cross-sections under different impacting disturbance loading levels were obtained. The paper is also to describe process of rock creep damage under disturbance loads and to explore the mechanism of micro-damage. The results have shown that rock failure is easy to happen suddenly rock is in or close to limit strength neighborhood during the process of disturbance. This will further lay the theory basis for the prediction of roadways' service life and evaluation of geotechnical engineering stability.

keywords: CT scanning, micro-damage, impacting disturbance, micro-crack, creep

Introduction

Surrounding rock of underground chambers are subjected to geo-stress or static stress, as well as under the dynamic loading in engineering practice. Due to excavation, bearing loads are quite great in deep mining; the surrounding rock is in high stress state. Within a certain range of chamber, rock is in or close to limit damage state. Dynamic loads were superimposed on them, will influence on stability of surrounding rock greatly.

Disturbance loads originate from blasting ,excavation and other engineering activities (shaft station, roadways haulage) vibration caused by these disturbance, its effect of mode is short time stress wave. Dynamic loads are random, such as frequency and intensity are uncertain, which compared with static loads, they are small.

Mechanical experiments are an efficient means of exploring the evolution law of internal damage during rock compression. The crack distribution on a rock surface in a certain stress state can be observed by optical or electronic microscope [1 – 3]. Furthermore, the crack distribution on an internal cross-section under a

¹Corresponding author. E-mail: fuzhiliang2007@yahoo.com.cn. College of Energy Resources and Safety , Anhui University of Science and Technology Huainan, Anhui 232001 , China

²Exploration & mining Center, Commonwealth Scientific and Industrial Research Organisation, Queensland 883,Australia

³School of Mechanics &Civil Engineering, China University of Mining & Technology, Beijing 100083, China

certain stress state can be established by using the computerized tomography (CT) technique [4 – 7]. Ref. [7 – 8] describes obtaining CT images by scanning the damaged rock specimen at a single given stage. That procedure cannot obtain real-time CT images at different stress stages during the full process of rock damage evolution. Analysis of CT values distribution and mathematical model of rock damage were made in details, relationship of CT value and rock damage variables is established [9 – 12].

Experiment

The rock was the tertiary gray green mudstone collected from the Beizao colliery under the sea, 5km far from Lngkou City in Shandong province, China (see Fig. 2).

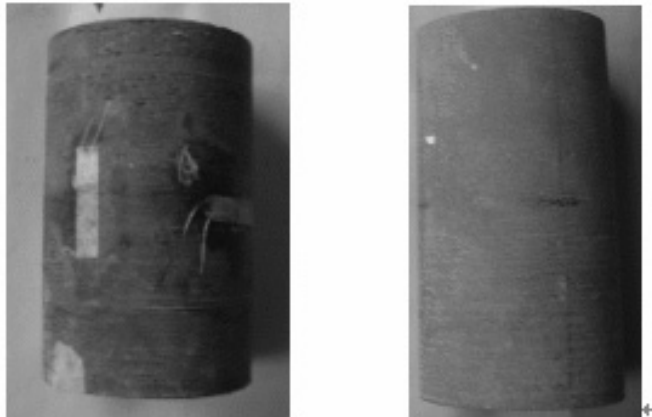


Figure 1: Grey green mudstone

The bulk density is 26.36 kN/m³; moisture content is 0.25%. The rock samples is processed into cylinder with size of diameter 50 mm and height 100mm(see Fig. 1) . Disturbance loop hanging from rock samples impacting on rock sample, mass of disturbance loop are 2.5kg, 5kg, 7.5kg and 10kg respectively . Load impulse dropping from different height were produced by different mass disturbance loop. Impact velocity is 4.75-4.87m/s. dropping height is 10cm-50cm. Impacting at same height until rock samples damage fully.

At present, effects of disturbance to rheology on different mass disturbance loop, there is still no theory and measure means to measure objects collision time accurately, so using disturbance load energy ΔW to express impacting load is more practically significant. Mass of disturbance impacting loop is M , dropping height is h . According to impulse theorem and energy theorem, ignoring energy consume, gravitational potential energy of disturbance loop impacting can be seen as convert-

ing into impulse, disturbance load energy of unit area ΔW is expressed as

$$\Delta W = \frac{M\sqrt{2gh}}{A} \tag{1}$$

where A is sectional area of samples (m^2); g is gravity acceleration, $g = 9.8 m/s^2$. Substituting data into formula (1)

$$\Delta W = 1566.59M\sqrt{h} \tag{2}$$

Table 1: Parameters of Impact disturbance energy

M/kg	H/cm	ΔW (J /s/ m^{-2})
5	15	2500
5	20	7500
5	20	10000
5	25	12500
5	30	15000
5	35	17500
5	40	20000

The tests have been conducted at the CT laboratory in University of Shandong science & technology and Shandong Coal sanatorium. The X-ray Spiral CT scanner, SIEMENS SOMATOM plus made in German and triaxial loading system developed by ourselves were used.

The space resolution of the CT machine is $0.35\text{ mm}\times 0.35\text{ mm}$, identifiable minimum volume is 0.12 mm^3 , density contrast resolution is 0.3%. The basic performance parameters of spiral CT are, voltage is 137 kV, electric current is 220 mA, scanning thickness is 0.1 mm, the amplification coefficient is 6.0.

Firstly put into the triaxial pressure cell, which is in turn put on the CT bed horizontally (the CT bed can be moved vertically or horizontally). Initial positioning and CT scanning of the rock samples is needed under no confining pressure. There are altogether five to ten scanning layers. The confining pressure is gradually increased up to 5MPa and then fixed. Then, the axial stress is applied with the given loading rate (the average loading rate is $0.1\times 10^{-3}\text{ mm/s}$) by stepping loading method until the specimen breaks. Real-time CT scanning for selected cross-sections has been conducted under different disturbed loading states. The scanning thickness is 10-20 mm (see Figs 2, 3 and 4.).

CT Scanning Images and Creep Deformation of Gray Green Mudstone

Micro-characteristics of gray green mudstone are shown in Fig .2. EMS pictures, , we can find that it was gray green, the crystal structure is dense, mudstone-like structure, micro pore development under the electron microscope with 300



Figure 2: Map of rock collecting resource

Table 2: Results of CT value and creep of rock specimen

Scan layer	Axial creep $\mu\epsilon \times 10^{-3}$	Lateral creep $\mu\epsilon \times 10^{-3}$	CT means	Disturbed energy (J/s)	note
1	0.0	0.0	2017.34	0.0	Initial
2	0.763	0.124	2027.98	986.7	Compression
3	0.855	0.221	2026.12	1356.8	Compression
4	2.062	0.527	2022.78	1621.5	Compression
5	3.295	0.802	2022.96	1752.3	Crack formation
6	4.489	1.049	2023.04	1967.1	Crack formation
7	5.803	1.375	2023.79	2073.2	crack propagation
8	7.038	1.680	2021.45	2337.8	crack propagation
9	8.135	3.084	1989.08	2510.6	crack propagation
10	9.319	5.582	1698.43	2704.4	Failure completely

times magnification; magnification is 1320; micro porosity of Interlayer is $5-20\mu\text{m}$, high porosity and permeability; magnification is 3300: flake clay is mainly composed of smectite, interlayer quartz, a little of leaf-shaped feldspars Crystal; The

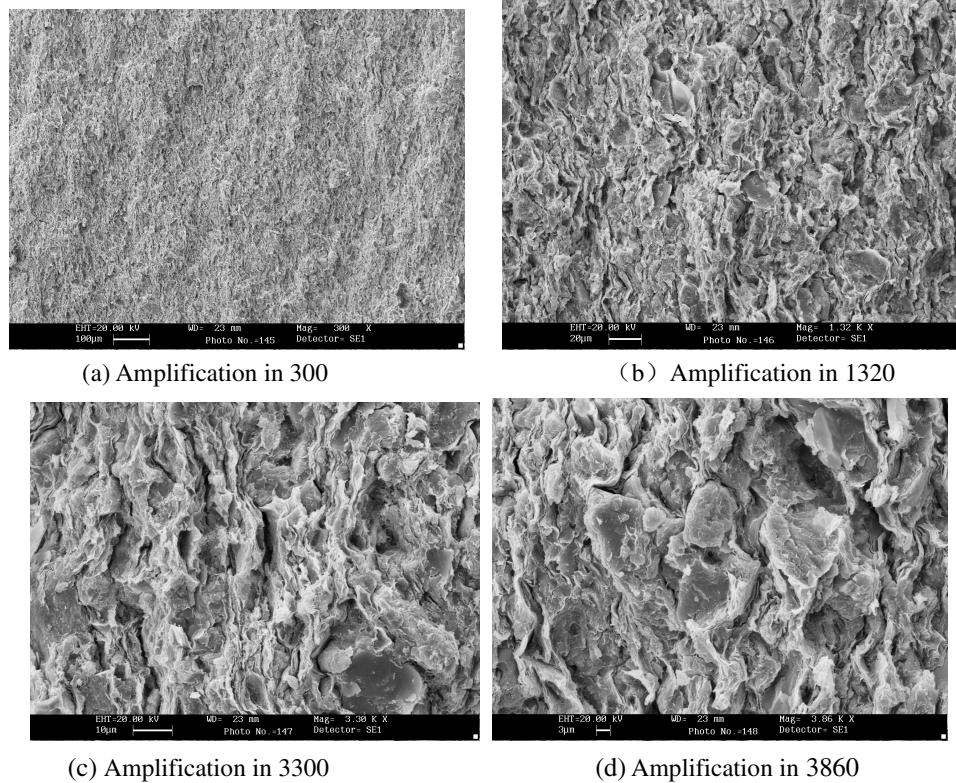


Figure 3: EMS picture of gray green mudstone

3860 times electron microscopy photos is intergranula, albite granule, granular Chlorite.

CT images can be divided into four evolution stages, namely uneven change stage of CT values ($\sigma_1=0-2.85\text{MPa}$, disturbance loads energy is in the range 0-2500 Joule). Five scanning cross sections have no apparent changes in this stage, The evolution law of CT number show that variance are similar in every point. Local crack evolution stage ($\sigma_1=2.85-4.59\text{MPa}$, disturbance loads energy is 7500 Joule). Rock samples enter into of state of cracks evolution on CT scale. Firstly low-density anomalous points appear in the upper right of CT-1; low density points occur under the CT-1 scanning layer, two points develop slowly, a zigzag ribbon distribution, which connect on CT-1 and CT-2 cross section, crack surface is parallel to the orientation of pressure stress. Penetrating cracks evolution stage ($\sigma_1=4.59-5.03\text{MPa}$, disturbance loads energy is over 10000 Joule). When σ_1 come to 6.59Mpa and disturbance loads energy is 15000 Joule, branching crack occur, which is perpendicular to original crack, two cracks vertical penetrate rock sample quickly, branching crack parallel to pressure, stress-strain curves are fluctuating.

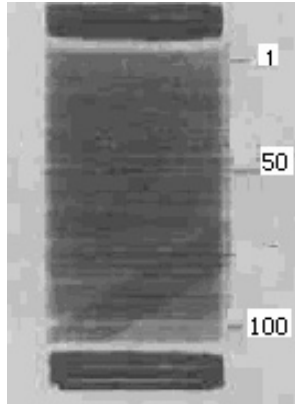


Figure 4: Grey green mudstone sample CT scan positioning lines

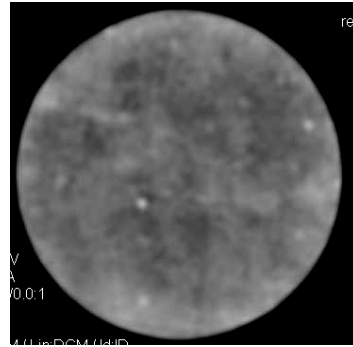


Figure 5: Grey green mudstone sample CT scan (unloaded)

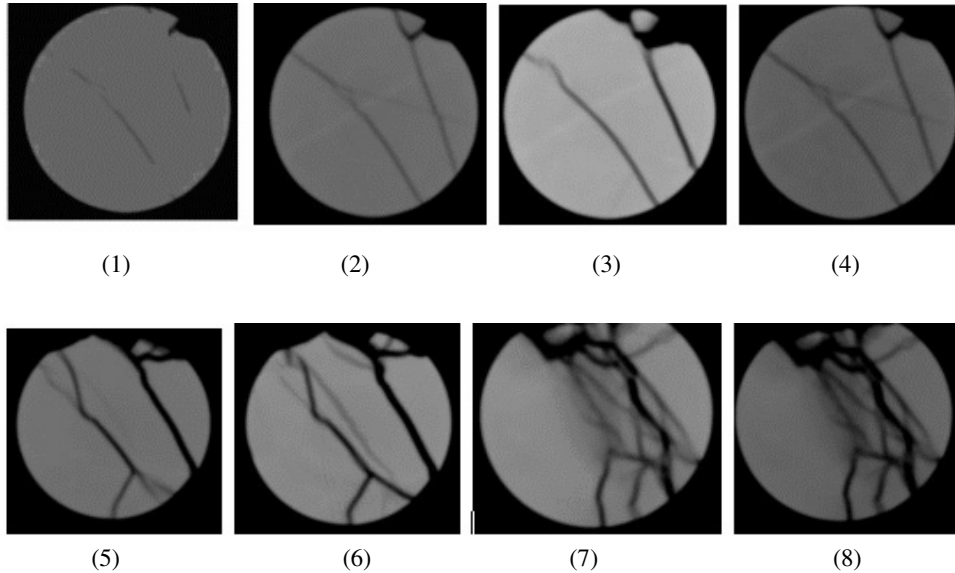


Figure 6: CT images of gray green mudstone of every scan section under different disturbing energy conditions (scanning layers from 1 to 8)

Subsequently, penetrating crack evolutes slowly, become wide along transverse direction, some irregular cracks emerge on CT-4 and CT-5 cross sections, and extend toward CT-2 and CT-3. When stress reach limit strength, if continue to apply disturbance loads, rock suddenly fail. According to failure modes, strength loss because failure sliding along the main crack plane.

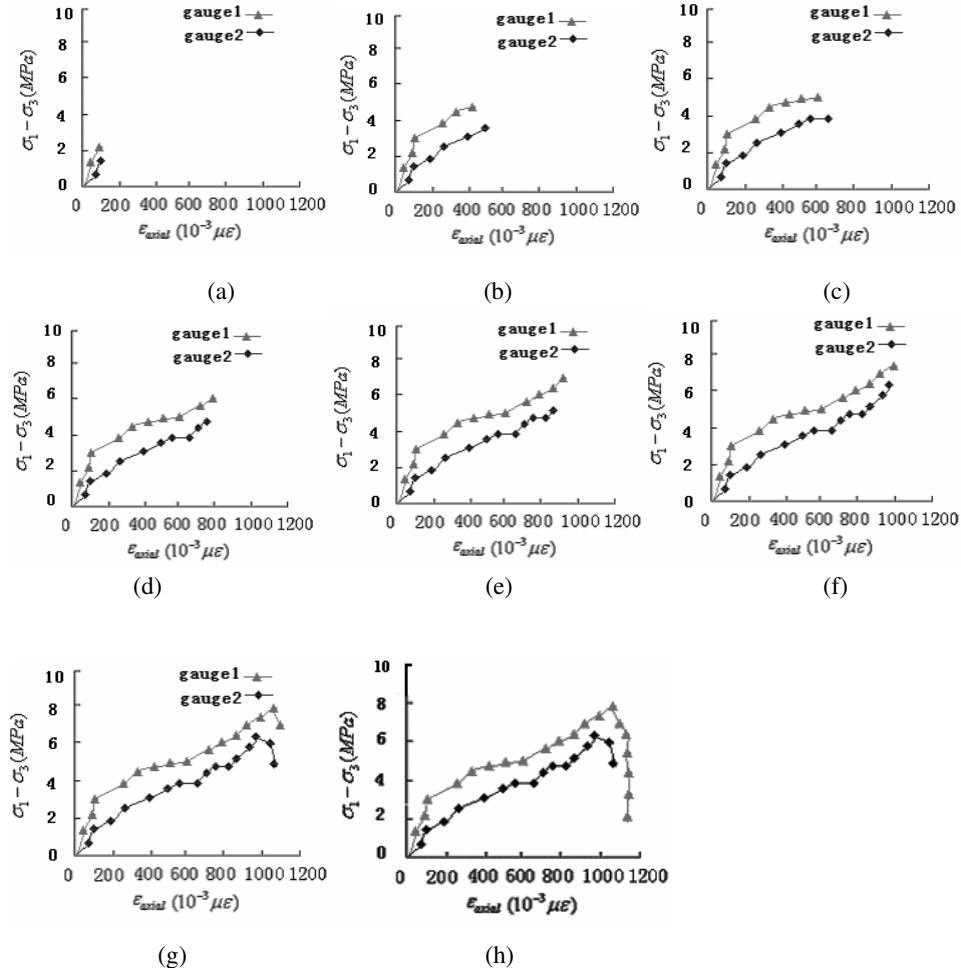


Figure 7: Axial creep curves of gray green mudstone of every scan section under different disturbing energy conditions (scanning layers from 1 to 8)

As far as the micro-structure is concerned, CT values of the first and second layer increase, pore decrease, but transverse swelling failure is more obviously in the third scanning layer. At the same time, CT variances of every layer increase. With the increase of disturbance loads, particles density reduce, pore increase in every layer, arrangement of rock particles and pore from initial disorganized to orientation. It is close to instability and failure stage of rock (fifth and sixth scanning layers). Rock fail fully after a transient pause phase (the seventh and eighth scanning layers).

The Damage Effects of Soft Rock under Disturbance Loads

Rock damage variable equation was represented by using CT values, according

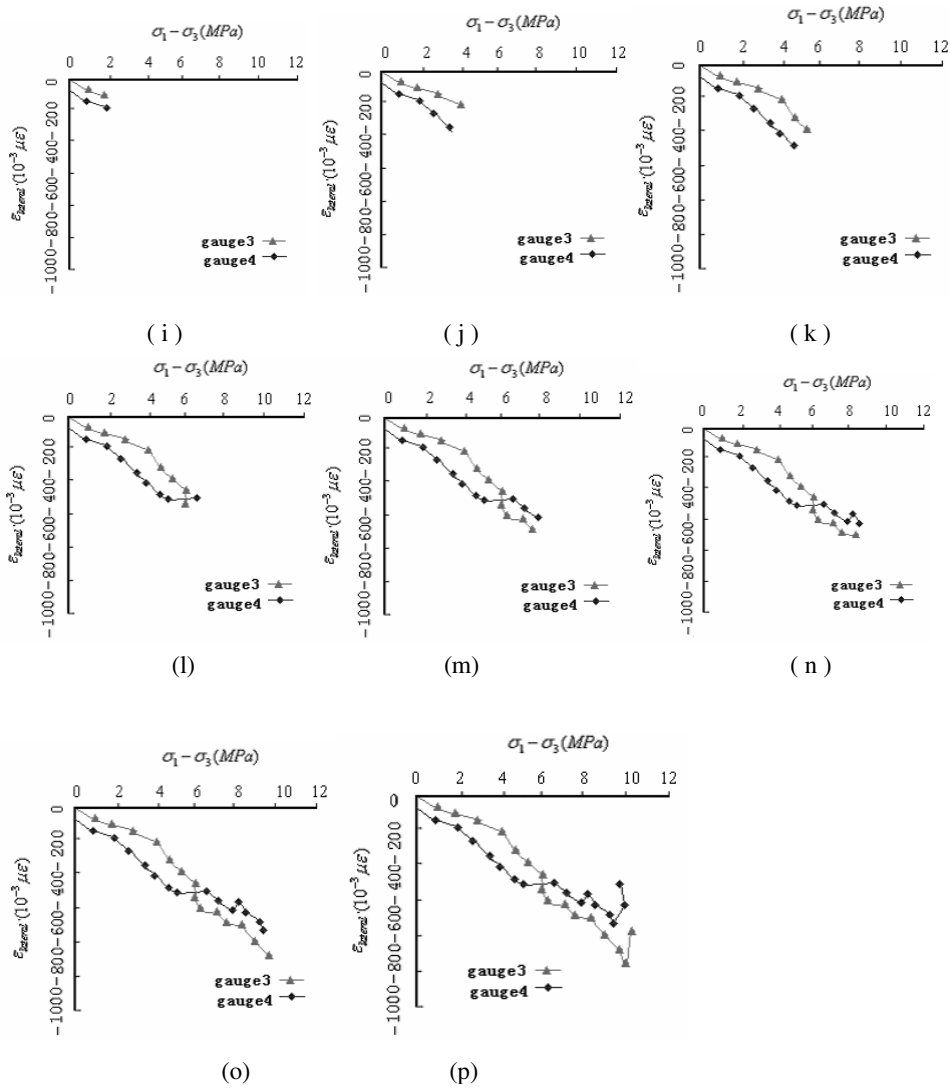


Figure 8: Lateral creep curves of gray green mudstone of every scan section under different disturbing energy conditions (scanning layers from 1 to 8)

Note: Figs. 1–8 Disturbance loads energy is 2500J, 5000J, 7500J, 10000J, 12500J, 15000J ,175000J and 2000J respectively.

to the reference literature ,the computation method^[13] is shown as following,

$$D_{creep} = \frac{1}{m_0^2 [H_0 - H_d] / (1000 + H_0)} \quad (3)$$

Where D_{creep} is creep damage variable rock under disturbance load, m_0 is the space

Table 3: Stress, creep and damage for grey green mudstone under triaxial loading condition

σ_1	—	0.0	0.2	0.4	0.6	0.8	1.0	1.2	1.4
σ_3/MPa									
axial		0.000	0.270	0.620	0.870	1.040	1.355	1.670	2.150
creep									
$\mu\varepsilon \times 10^{-6}$									
D_{creep}		0.16547	0.17162	0.17418	0.17879	0.17930	0.17930	0.18186	0.28739

Table 4: Calculation results of creep damages for rock under the disturbance impact load

S-1		S-2		S-3	
CT means /Hu	Damage level	CT means /Hu	Damage level	CT means /Hu	Damage level
1333.9	0.0	1345.9		1365.9	
1334.7	0.0	1345.7		1367.7	
1337.2	0.0	1350.2		1368.2	
1346.8	0.0	1351.8	0.0	1385.8	0.0
1341.2	0.020	1352.2	0.022	1490.2	0.034
1325.9	0.074	1349.9	0.069	1501.9	0.068
1306.8	0.142	1347.8	0.172	1523.8	0.214
1282.8	0.227	1314.8	0.247	1497.8	0.257
1247.1	0.354	1306.1	0.384	1485.1	0.384
1198.4	0.572	1298.4	0.602	1468.4	0.542

resolution of CT machine, the CT value of the initial rock density is H_0 , H_d is the CT value of the damage rock density during the disturbance load process of rock material.

Damage variables of different damage development stages under triaxial compression were calculated by Eq (3), they are given in Table 3.

Stress, strain and damage variables at different damage development stages were given in Table 3.

Axial strain increase with stress increase under triaxial compression for every sample. With the extension of damage, the strain and stress increase and the damage variables increases accordingly.

According to Tables 2 to 4, when CT mean values decrease with disturbance loads increase, creep damage level begin to increase. It shows that rock sample is compacted, new micro fissure and holes occur. Continue to apply disturbance load, micro-cracks increase continuously, and they extend from center to circumference

explosively, finally, rock lose bearing capacity. From rock appearance, it find that rock uneven deformation and local swell occur in this stage. Damage occur on local swell.

The relationship curves of cross-section density damage, disturbance load and axial strain were shown in Fig 9.

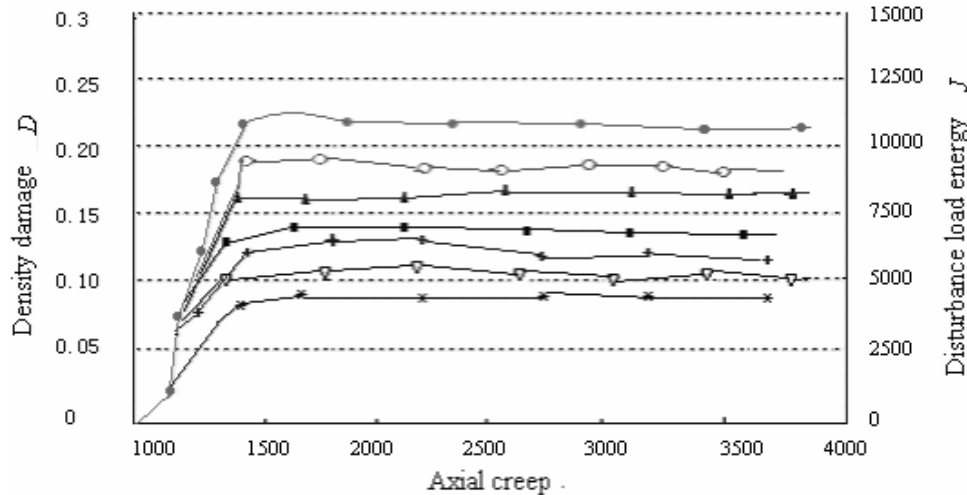


Figure 9: Relationship of density damage increment, axial creep and disturbance load energy of every scanning cross section of grey green mudstone

Seen from Fig 9, we can conclude that density damage increment D in seven scanning layers increased or decreased as axial stress and disturbance load energy increased, corresponding to rock compacting and dilatancy, respectively. When CT-1 scanning cross section come into dilation stage, other scanning cross sections are still compacting, it means there is partial dilation in whole compacting stage. The inflection points of Curve D are transition points of densification and dilatancy, corresponds to images of D . Images show that macro-crack is generating, and extend from upper to down. Rock dilatancy is the essence of crack strengthening cause local volume to swell. CT dimension crack initiate on dilatancy location. Densification quantity are large on the stages of confining pressure is exerted and initial compacting, rock pore is big, rock properties are soft. It is transient dilatancy stage. In the early evolution phase of CT dimension crack, curve is straight, swell effect caused by longitudinal compression and transverse expansion was cancelled. At the late evolution phase of CT dimension crack, density damage increment reduce due to cracks extend obviously.

Conclusion

Testing results have shown that when axial load come into limit strength neigh-

borhood, rock micro crack link into larger crack, creep rate increase quickly in a short time, larger plastic deformation occur; this is called as disturbance accelerating creep stage. When rock is within limit strength neighborhood, rock begin with creep micro-damage under smaller disturbance load(disturbance energy is 2500J-5000J). If disturbance load is larger, directly enter into disturbance accelerating creep stage, failure occur instantaneity.

Acknowledgement

Funding by: National Nature Science Funds committee (No. 50474029).

References

1. Ren, Jian-xi (2001): Realime CT Monitoring for the Meso-Iamage Propagation Characteristics of Rock Under Triaxial Compression[J]. *Journal of Experimental Mechanics* 16(4):387-394.
2. Fu, Zhi-liang (2007): Theoretical and experimental study on effects of disturbance to rock creep and damage characteristics [D].Doctorate Dissertation of Shandong University of Science and Technology.
3. Kawakata, H.; Cho, A.; Kiyama, T. et al (1999): Three-dimensional observations of faulting process in Westerly granite under uniaxial and triaxial condintions by X-ray CT scan. *Tectonophysics* (313):293-305.
4. KawaKata, H.; Cho, A.; Yanagidani, T. et al. (1997): The observations of faulting in Westerly granite under triaxial compression by X-ray CT scan. *Int. J. Rock Mech, Sci.* 34(34):151-162.
5. Feng, Xia-Ting; Chen, Sili et al (2004): Real-time computerized tomography (CT) experiments on sandstone damage evolution during triaxial compression with chemical corrosion. *International Journal of Rock Mechanics and Mining Sciences* 41(2):181-192.
6. Li, Shucui; Li, Shuchen; Zhu, Weishe et al. (2004): CT real-time testing study on effect of water on crack growth in fracturedrock mass[J]. *Chinese Journal of Rock Mechanics and Engineering* 23(21):3584-3590.
7. Yang, Gengshe; Ie, Dingyi; Zhang, Changqing et al (1996): CT identification of rock damage properties[J]. *Chinese Journal of Rock Mechanics and Engineering* 15(1):48-54.
8. Li, Shucui; Li, Tingchun; Wang, Gang; Bai, Shiwei (2007): The CT real-time scanning tests of the rock specimens with artificial initial crack under unaxial conditions[J]. *Chinese Journal of Rock Mechanics and Engineering* 26(3):484-492.
9. Chen, Si-li,Feng, Xia-ting, Zhou, Hui (2004): Study on triaxial meso-failure

mechanism and damage variables of sandstone under chemical erosion[J]. *Rock and soil mechanics* 25(9):1363-1367.

10. Helman, G. T. (1985): *From Projection to Reconstruct Images—Theory Foundation of Computerized Tomography[M]*. Translate by Yan Hongfan, Beijing: SciencePress.
11. Ge, Xiurun; Ren, Jianxi; Pu, Yibin et al (1999): A real-in-time CT triaxial testing study of meso-damage evolution law of coal[J]. *Chinese Journal of Rock Mechanics and Engineering* 18(5):497-502.
12. Ren, Jian-xi (2004): Real-time computerized tomography(CT) test of failure process of jointed granite under unloading in three gorges project(TGP)[J]. *Journal of Coal Science & Engineering* 10(2):11-14.